Nonlinear Breit-Wheeler pair creation with bremsstrahlung ? rays

Downloaded from: https://research.chalmers.se, 2022-01-28 23:01 UTC

Citation for the original published paper (version of record):
Blackburn, T., Marklund, M. (2018)
Nonlinear Breit-Wheeler pair creation with bremsstrahlung ? rays
Plasma Physics and Controlled Fusion, 60(5)
http://dx.doi.org/10.1088/1361-6587/aab3b4

N.B. When citing this work, cite the original published paper.

research.chalmers.se offers the possibility of retrieving research publications produced at Chalmers University of Technology.
It covers all kind of research output: articles, dissertations, conference papers, reports etc. since 2004.
research.chalmers.se is administrated and maintained by Chalmers Library

(article starts on next page)

OPEN ACCESS
IOP Publishing
Plasma Physics and Controlled Fusion
Plasma Phys. Control. Fusion **60** (2018) 054009 (8pp)
https://doi.org/10.1088/1361-6587/aab3b4

Nonlinear Breit–Wheeler pair creation with bremsstrahlung γ rays

T G Blackburn and M Marklund

Department of Physics, Chalmers University of Technology, SE-41296 Gothenburg, Sweden

E-mail: tom.blackburn@chalmers.se

Received 29 December 2017, revised 9 February 2018
Accepted for publication 2 March 2018
Published 22 March 2018

Abstract

Electron–positron pairs are produced through the Breit–Wheeler process when energetic photons traverse electromagnetic fields of sufficient strength. Here we consider a possible experimental geometry for observation of pair creation in the highly nonlinear regime, in which bremsstrahlung of an ultrarelativistic electron beam in a high-Z target is used to produce γ rays that collide with a counter-propagating laser pulse. We show how the target thickness may be chosen to optimize the yield of Breit–Wheeler positrons, and verify our analytical predictions with simulations of the cascade in the material and in the laser pulse. The electron beam energy and laser intensity required are well within the capability of today's high-intensity laser facilities.

Keywords: positron production, colliding beams, strong-field QED

(Some figures may appear in colour only in the online journal)

1. Introduction

Breit–Wheeler pair creation is an elementary process of quantum electrodynamics (QED) in which matter and antimatter are produced purely from light [1]. The two-photon, or linear, process has yet to be detected experimentally, as it is difficult to achieve a collision between photon beams where the flux is sufficiently high and the per-particle centre-of-mass energy exceeds twice the electron mass. Both these requirements have been met experimentally, and pair creation observed, in the multiphoton regime: [2] used Compton scattering of a 46.6 GeV electron beam in a laser pulse with strength parameter $a_0 = 0.36$ to produce γ rays that subsequently interacted with further laser photons to produce electron–positron pairs [3]. Here $a_0 = eE/(m\omega_0)$ is the classical nonlinearity parameter for an electromagnetic wave with electric field amplitude E and angular frequency ω_0 [4]. e and m are the electron charge and mass respectively. (Natural units $\hbar = c = 1$ are used throughout this paper.)

In this work we consider Breit–Wheeler pair creation in the highly nonlinear regime $a_0 \gg 1$, which is relevant for the study of astrophysical plasmas in strong magnetic fields [5] and is expected to occur prolifically in the next generation of high-intensity laser experiments [6]. Prospects are good for experimental exploration of this regime with currently existing laser facilities, due to advances in laser wakefield acceleration (LWFA) [7] and increases in available laser power. It is now possible to accelerate electrons to multi-GeV energies in relatively compact setups [8–10] and to focus laser pulses to intensities $>10^{22}$ W cm^{-2} [11, 12]. Combining these lets us study the dynamics of energetic particles in electromagnetic fields of unprecedented strength using 'all-optical' designs [13]. Indeed, evidence of radiation reaction (recoil due to photon emission) in the collision of a LWFA electron beam with an intense laser pulse has recently been reported [14, 15].

The configuration we study is the collision of GeV γ rays with a laser pulse that has $a_0 > 10$. A possible experimental realization of this is illustrated in figure 1, following [16]. The γ rays are created by bremsstrahlung of a LWFA electron beam in a high-Z target; the ultrashort, energetic γ ray bunches this produces already find applications in imaging and radioisotope generation (see [17, 18] and references therein). A gap is introduced between the solid target and point of collision with the laser to permit magnetic deflection of the source electrons and electron–positron pairs produced inside

Original content from this work may be used under the terms of the Creative Commons Attribution 3.0 licence. Any further distribution of this work must maintain attribution to the author(s) and the title of the work, journal citation and DOI.

 © 2018 IOP Publishing Ltd Printed in the UK

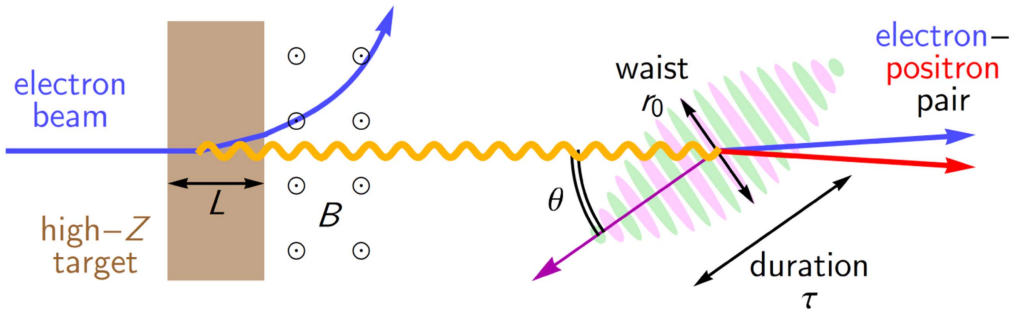

Figure 1. An ultrarelativistic electron beam, produced by laser wakefield acceleration (not shown), strikes a high-Z target. The bremsstrahlung γ rays so produced are separated from the charged components of the cascade by magnetic deflection, and collide downstream with an intense laser pulse. Here they produce electron–positron pairs via the nonlinear Breit–Wheeler process.

the target, ensuring that we have a pure light-by-light collision.

The importance of QED effects is measured by the parameter [19]

$$\chi_\gamma = \frac{a_0 \omega_0 \omega (1 + \cos\theta)}{m^2}, \tag{1}$$

where ω is the photon energy, a_0 and ω_0 are the laser strength parameter and frequency, and θ is the collision angle between the two (see figure 1). The onset of pair creation (approximately one pair per pC of electrons in this geometry) occurs for $\chi_\gamma \gtrsim 0.1$, or when $(\omega/\mathrm{GeV})(a_0/20) \gtrsim 1$ at a wavelength of 0.8 μm.

Using bremsstrahlung to produce the seed photons, rather than Compton scattering in a direct collision between electron beam and laser pulse [20], is motivated by the breadth of the energy spectrum [21]. As it extends up to the initial energy of the electron, using GeV electron beams will produce the GeV photons that are necessary for $\chi_\gamma \gtrsim 0.1$. Photons of this energy could also be used to study the linear Breit–Wheeler process, either by colliding the γ rays with the high-temperature x-ray bath in a laser-irradiated hohlraum [22], or by colliding two such beams directly [23]. They could also be used to seed QED avalanches at intensities $>10^{23}$ W cm^{-2} [24].

By using a laser pulse with $a_0 > 10$ as the target, we enter the strong-field regime where the pair creation probability increases non-perturbatively with the laser amplitude. This will permit the positron yield to be substantially higher than reported by [2] despite the lower electron beam energies we consider. To show this, we first calculate an estimate for the pair creation probability in section 2 and then show that bremsstrahlung is a good source of sufficiently energetic photons in section 3. Then we combine these two to estimate the number of pairs per electron in section 4. We find that the thickness of the high-Z target may be chosen to maximize the number of positrons that are produced in the laser pulse and discuss the importance of reducing the divergence of the γ ray beam.

2. Probability of Breit–Wheeler pair creation

We begin by determining an analytical estimate for the probability that an electron–positron pair is created when a photon with energy ω collides with a laser pulse that has $a_0 \gg 1$. We employ the locally constant field approximation (LCFA) [19], using probability rates that are calculated in an equivalent system of fields in which the local value of χ is the same [25, 26]. This requires $a_0^3/\chi \gg 1$, as will always be the case here [27]. (See [28–31] and references therein for a discussion of how the pair creation probability may be calculated exactly in the framework of strong-field QED.)

While the χ parameter, which determines the importance of QED effects, would be maximized for a head-on collision between photons and laser pulse, we show in figure 1 a crossing angle $\theta > 0$. This is likely to be unavoidable in future laser experiments, as it prevents damage to the focussing optics by transmitted light and high-energy particles; collision angles of 15° and 30° are envisaged in [16]. It is necessary therefore to take the transverse structure of the focussed laser pulse into account when calculating the positron yield, as the distance over which the γ rays are exposed to the strong fields depends upon both the laser's temporal duration and focal spot size.

Recent studies of strong-field QED processes in focussing laser fields include: exact calculation from QED of the pair creation probability for the head-on collision of a photon and a tightly-focussed laser pulse [32]; and determination of the intensity threshold for a pair cascade to be launched by two counter-propagating, tightly-focussed laser pulses [33]. In both cases a description of the electromagnetic field that goes beyond the paraxial approximation is used, e.g. [34].

While this captures the angular divergence of a tightly-focussed laser pulse, the transverse intensity profile measured at the focal plane is rarely so ideal [35]. To capture the essential physics in our analytical calculation, we consider the laser pulse to be a 'light bullet' with Gaussian transverse intensity profile of constant size. The duration of the pulse, defined as the full width at half maximum (FWHM) of the temporal intensity profile, is given by τ. The radius of the beam is given by r_0, the distance over which intensity falls to $1/e^2$ of its central value. We expect that additional effects, such as the finite size of the γ ray beam and spatiotemporal

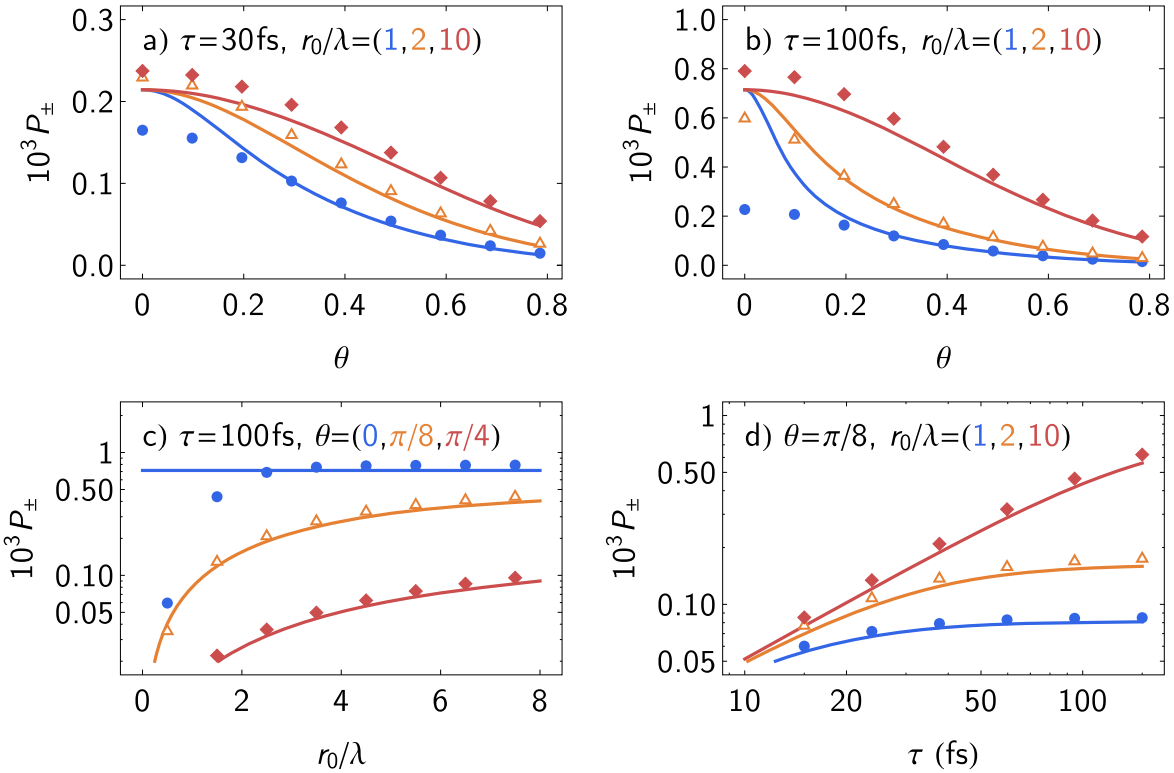

Figure 2. The probability of pair creation $P_\pm$ in the collision of a γ ray with energy $\omega = 1000$ m and laser pulse with $a_0 = 30$ and wavelength 0.8 μm, as a function of the crossing angle θ, the laser (FWHM) duration τ and focal spot size r_0: (lines) from (4) and (points) numerical integration.

offsets, may be accounted for approximately by modifying the effective peak amplitude a_0 [36].

The quantum nonlinearity parameter at time t of a photon with energy ω colliding with a linearly-polarized laser pulse with normalized amplitude a_0 and angular frequency ω_0 at crossing angle θ is

$$\chi_\gamma = \frac{a_0\omega_0\omega(1+\cos\theta)}{m^2}|\sin\phi|\exp\left(-\frac{\ln 2\,\phi^2}{2\pi^2 n_{\rm eff}^2}\right), \qquad (2)$$

where $\phi = (1+\cos\theta)\omega_0 t$ and

$$n_{\rm eff} = \frac{\omega_0\tau}{2\pi}\left[1+\frac{\tau^2\tan^2(\theta/2)}{r_0^2\ln 4}\right]^{-1/2} \qquad (3)$$

is the number of wavelengths that characterizes the effective pulse duration.

Integrating the probability rate for pair creation from [25] over the trajectory specified by (2), using the same saddle-points method as [20], we find that the pair creation probability

$$P_\pm \simeq \alpha a_0 n_{\rm eff}\mathcal{R}\left[\frac{a_0\omega_0\omega(1+\cos\theta)}{m^2}\right], \qquad (4)$$

where α is the fine-structure constant, $n_{\rm eff}$ is as given in (3) and

$$\mathcal{R}(x) = \frac{0.453K_{1/3}^2(\frac{4}{3x})}{1+0.145x^{1/4}\ln(1+2.26x)+0.330x} \qquad (5)$$

as in [20]. The argument of $\mathcal{R}$ in (4) is the peak χ_γ of the photon.

This analytical scaling may be verified against numerical integration of the pair creation rate. In the latter we explicitly account for the effects of tight focussing and model the spatial dependence of the pulse as a Gaussian beam of spot size r_0 and Rayleigh range $z_{\rm R} = \pi r_0^2/\lambda$. The fields are calculated to fourth-order in the diffraction angle $\epsilon = r_0/z_{\rm R}$, i.e. beyond the paraxial approximation [34]. The temporal envelope of the pulse remains a Gaussian with FWHM duration τ. For definiteness, we fix the γ-ray energy $\omega = 1000$ m and the laser $a_0 = 30$ at a wavelength $\lambda = 0.8$ μm, which corresponds to a peak intensity of 2×10^{21} W cm^{-2}. The pair creation probability predicted by (4) is compared to the numerical results for varying collision angle θ, pulse duration τ and focal spot size r_0 in figure 2.

Figures 2(a) and (b) show that the pair creation probability is maximized for a head-on collision and decreases with increasing collision angle. This is because both χ_γ and $n_{\rm eff}$ are reduced for $\theta > 0$ (in the latter case, because $r_0 < \tau$). The two effects may be separated by comparing the results for different spot sizes: at $r_0 = 10\lambda$ (in red), the pulse is effectively a plane wave and the decrease in $P_\pm$ is entirely due to the geometric dependence of χ_γ.

We expect that agreement between the analytical and numerical results should be better for larger spot sizes, because we assumed a plane wave in deriving (4). Our scaling does capture with good accuracy the dependence of the pair creation probability on collision angle for the 2λ and 10λ

spots. However, for the case that $r_0 = \lambda$, there is good agreement only if $\theta \gtrsim 0.2$. Otherwise the analytical result overestimates $P_\pm$ ($\theta = 0$) by 30% if the pulse duration is 30 fs or 210% if it is 100 fs.

This error arises when the pulse duration τ becomes larger than the confocal parameter $2z_\mathrm{R}$, as the probe photon can then 'observe' the variation in intensity caused by the contraction and expansion of the laser pulse as it passes through focus; were $\tau \ll 2z_\mathrm{R}$ instead, this variation would be small compared to that of the pulse temporal envelope.

We can therefore place a limit on the validity of (4) in terms of the effective number of cycles n_eff (defined by (3)):

$$n_\mathrm{eff} < 2\pi(r_0/\lambda)^2. \tag{6}$$

Alternatively, this may be expressed in terms of a minimum angle:

$$\theta > \theta_\mathrm{min}, \quad \tan^2\left(\frac{\theta_\mathrm{min}}{2}\right) = \ln 4\left[\left(\frac{\lambda}{2\pi r_0}\right)^2 - \left(\frac{r_0}{\tau}\right)^2\right]. \tag{7}$$

Evaluating this for $\tau = 100$ fs, we find that $\theta_\mathrm{min} = (0.36, 0.14, 0)$ for $r_0/\lambda = (1, 2, 10)$ respectively. Inspection of figure 2(b) shows that these bounds are consistent with the minimum angles for which our analytical scaling agrees with the numerical results.

We may further use (7) to determine the smallest spot size at given collision angle for which our analytical scaling is valid. For the range of angles $\theta = (0, \pi/8, \pi/4)$, we find $r_0/\lambda = (2.4, 0.93, 0.45)$. This is in good agreement with the results shown in figure 2(c), where we compare the pair creation probability as a function of spot size at fixed pulse duration.

Finally, we show results with fixed $\theta = \pi/8$ and varying pulse duration in figure 2(d). The minimum spot size at this collision angle is $r_0/\lambda = 0.93$, so we find excellent agreement between our analytical predictions and the numerical results across the explored parameter range.

Having verified its accuracy, we are now in a position to apply our analytical result to the case that the high-energy photons are generated by bremsstrahlung, as shown in figure 1.

3. Bremsstrahlung photon generation

The pair creation probability (4) is strongly suppressed for $\chi_\gamma \ll 1$. Reaching $\chi_\gamma \sim 1$ with the intensities that may be reached with today's high-intensity lasers ($\sim 10^{21}$ W cm^{-2}), requires photon energies in the GeV range [20]. We now turn to how bremsstrahlung of an ultrarelativistic electron beam in a high-Z material may be used as the source of such photons. In particular, we will use our analytical results to show how the bremsstrahlung process may be optimized to produce the greatest number of Breit–Wheeler positrons. While these results are not dependent on the source of the electrons, one advantage of using LWFA is the small size and divergence of the accelerated electron beam [37]. As the γ ray beam inherits this size and divergence, this aids the achievement of good overlap with the second laser pulse, which must be focussed to a micron-sized focal spot to reach high intensity [14]. Although high energy γ rays may also be produced via direct illumination of a solid target with an intense laser [38–40], the characteristic energy is lower (100s MeV) and the divergence larger [18].

For the ultrarelativistic particles under consideration here, the two processes that dominate the evolution of an electromagnetic cascade within the material are bremsstrahlung photon emission and Bethe–Heitler pair creation. These occur when electrons (or positrons) and photons respectively interact with the Coulomb fields of individual heavy atoms. To a good approximation, the effect of the material properties, such as atomic number Z and mass density ρ, on the bremsstrahlung spectrum may be parametrized by using only its radiation length L_rad.

Under the approximations of complete screening and vanishing target thickness, the number of photons produced with fractional energy $f = \omega/E_0$ is

$$\frac{\mathrm{d}N_\gamma}{\mathrm{d}f} \simeq \frac{\ell}{f}\left(\frac{4}{3} - \frac{4f}{3} + f^2\right), \tag{8}$$

where $E_0 \gg m$ is the initial energy of the electron and $\ell = L/L_\mathrm{rad}$, the target thickness L scaled by the radiation length [41]. Equation (8) neglects attenuation of the photon beam due to pair creation within the solid target, thereby overestimating the high-energy tail of the spectrum even for $\ell \simeq 0.01$. This is particularly important here because the contribution to the Breit–Wheeler positron yield will be dominated by the highest-energy photons. A good approximation to attenuated bremsstrahlung spectrum for target thicknesses $0.5 \lesssim \ell \lesssim 2$ is given by [21]

$$\frac{\mathrm{d}N_\gamma}{\mathrm{d}f} \simeq \frac{(1-f)^{4\ell/3} - e^{-7\ell/9}}{f\left[\frac{7}{9} + \frac{4}{3}\ln(1-f)\right]}. \tag{9}$$

We compare (8) and (9) to the results of GEANT4 simulations [42–44] for electrons with $E_0 = 2$ GeV striking lead targets of various thicknesses in figure 3(a). (The radiation length of lead $L_\mathrm{rad} = 5.6$ mm.) For simplicity we assume that the electron beam is pencil-like (i.e. all electrons propagate perpendicular to the target surface) and monoenergetic. The latter is justified even though LWFA electron beams have broad energy spectra, as it is the yield of the highest energy photons that is important for Breit–Wheeler pair creation. Therefore it is necessary to simulate the interaction only for the high energy component of the electron beam. We find that the photon spectra are broad, with substantial emission of γ rays with energy greater than 1 GeV. While the general shape of the spectrum at $L = 0.2$ mm is captured well by (8), it is not very accurate near $f \simeq 1$. For thicker targets, (9) gives better predictions in the range $f > 0.5$, particularly for photons near the bremsstrahlung tip. This will prove significant when we estimate the positron yield analytically, as this is dominated by the highest-energy photons.

Due to the ultrarelativistic nature of the incident electrons, the emitted photons are well-collimated around the forward direction: figure 3(b) shows that for $L = 2$ mm

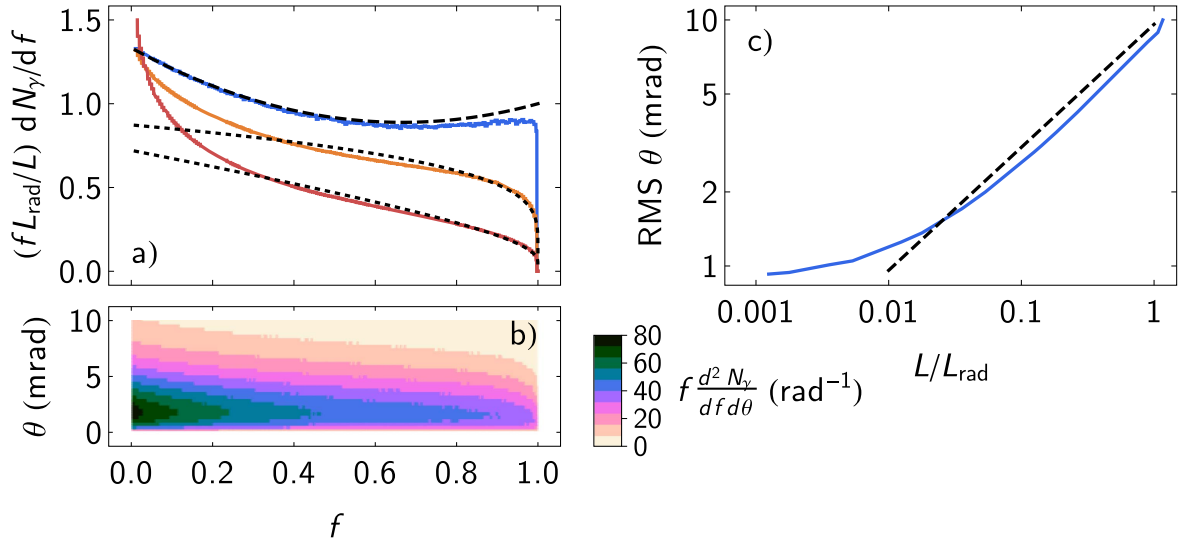

Figure 3. Bremsstrahlung photon generation when a 2 GeV electron beam strikes a lead target of thickness L: (a) energy spectra from (solid) simulations, (dashed) (8) and (dotted) (9) for $L = 0.2$ mm (blue), 2 mm (orange) and 5 mm (red); (b) energy-divergence spectrum for $L = 2$ mm; (c) the root-mean-square divergence of photons with $f > 0.5$ from (solid) GEANT4 simulations and (dashed) (10).

($\ell = 0.36$) the typical divergence is 5 mrad and narrows slightly with increasing photon energy. Relativistic beaming means that we expect the divergence of the bremsstrahlung photons to be inversely proportional to the Lorentz factor of the electron beam: for $\ell \sim 1$, the root-mean-square (rms) angle is approximately [37]

$$\theta_{\rm rms} \simeq \frac{\sqrt{\ell}}{[E_0/(19.2\ {\rm MeV})]}. \tag{10}$$

A comparison with simulation results shown in figure 3(c) shows that this scaling works reasonably well.

We now discuss the implications of these results for the generation of Breit–Wheeler pairs. The divergence of the γ ray beam will play an important role because it means that the beam will undergo transverse broadening as it propagates over the distance between the high-Z target and the focal plane of the secondary laser pulse (see figure 1). This reduces the number of γ rays that actually hit the region of highest intensity and so the positron yield. (It would also alter the pair creation probability even for those photons that do hit the pulse, as χ_γ depends on θ. However, for milliradian-level shifts, this is a relatively small effect compared to that of the reduced overlap.)

Assuming a divergence given by (10), the fraction of photons R that hit the focal spot (size r_0) after propagating a distance D may be estimated as

$$R \simeq 3 \times 10^{-5} \frac{(E_0/{\rm GeV})^2 (r_0/\mu{\rm m})^2}{\ell (D/{\rm cm})^2}. \tag{11}$$

The importance of this reduction becomes clear when we consider that $P_\pm \sim 10^{-4}$ (at $\tau = 30$ fs, see figure 2). The number of γ rays emitted per electron incident on the solid target is of order one for $L \sim L_{\rm rad}$. Thereby estimating $N_\gamma \sim 10^9$ for a beam charge of 100 pC, we find that (11) reduces the positron yield from 10^5 to only one. A possible way to overcome this would be to focus the electron beam with a quadrupole magnet before it strikes the heavy target, compensating for the increase in divergence during development of the cascade [16], and the intrinsic divergence of the electrons (a few mrad in size for LWFA [7]).

The more positive result is that the photons produced in bremsstrahlung are sufficiently hard that they can used to probe nonlinear Breit–Wheeler pair creation. Equation (9) predicts that the number of photons per electron with $f > 0.5$ is as large as $N_\gamma/N_e \simeq 0.2$ for $\ell \simeq 1$. Thus for electron beam energies in excess of a GeV, as are available from LWFA, we can expect a large number of photons with χ_γ sufficient for pair creation to take place within a high-intensity laser. Successful identification of this signal in an experiment requires careful control of the background. The most important contribution to this comes from Bethe–Heitler pair creation within the solid target. As is shown in figure 4, this generates a collimated beam of positrons with energies comparable to the initial electrons', which must be deflected away from the laser focal spot. This could be accomplished with a permanent magnet with field strength B and length d placed after the solid target (see figure 1), which would deflect a positron with energy E_+ by an angle $\theta[^\circ] \simeq 1.7B[{\rm T}]d[10\ {\rm cm}]/E_+[{\rm GeV}]$. These background positrons can be distinguished from the Breit–Wheeler positrons, which we discuss next, given single-particle detectors with sufficient angular (mrad) and temporal (picosecond) sensitivity [16].

4. The positron yield and optimal target thickness

The number of electron–positron pairs, per electron of the incident beam, may be estimated by integrating the bremsstrahlung spectrum weighted by the pair creation probability (4):

$$N_\pm \simeq \alpha a_0 n_{\rm eff} \mathcal{B}(\ell, \chi_e). \tag{12}$$

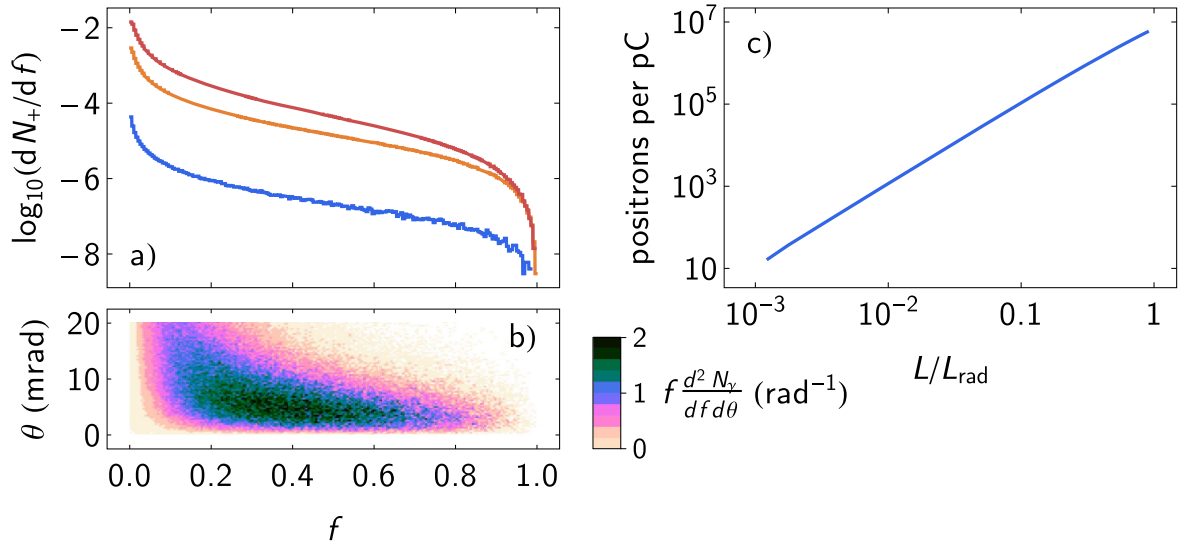

Figure 4. Bethe–Heitler positron generation when a 2 GeV electron beam strikes a lead target of thickness L: (a) energy spectra for $L = 0.2$ mm (blue), 2 mm (orange) and 5 mm (red); (b) energy-divergence spectrum for $L = 2$ mm; (c) and the number of positrons per pC of charge in the incident electron beam, all from GEANT4 simulations.

Here we have defined an auxiliary function $\mathcal{B}$ to absorb the positron yield's dependence on the properties of the solid target:

$$\mathcal{B}(\ell,\,\chi_e) = \int_0^1 \mathcal{R}(f\chi_e)\frac{\mathrm{d}N_\gamma}{\mathrm{d}f}\,\mathrm{d}f. \tag{13}$$

By using (8) or (9) for $\mathrm{d}N_\gamma/\mathrm{d}f$, $\mathcal{B}$ becomes a function of only two parameters: ℓ, the scaled target thickness, and $\chi_e = E_0 a_0 \omega_0 (1+\cos\theta)/m^2$. The former encapsulates the material properties through L_{rad}. The latter would be the quantum parameter of the electron, if it, rather than its photons, collided with the laser pulse. It depends upon the initial energy of the electron beam E_0, the normalized amplitude a_0 and angular frequency ω_0 of the intense laser pulse, and the crossing angle θ between the two.

Let us first consider the case where $\ell \ll 1$, so that we may use (8) for the photon spectrum. It is evident that the number of positrons increases linearly with target thickness, as the number of bremsstrahlung photons does as well. In the limit that $\chi_e \ll 1$, the integral in (13) may be performed analytically, with the result $\mathcal{B} = \frac{3}{8}\ell\chi_e\mathcal{R}(\chi_e)$. Otherwise, the integral must be performed numerically. A fit to these results, accurate to 5% over the range $0.01 < \chi_e < 10$ is

$$\mathcal{B}(\ell,\,\chi_e) \simeq \frac{0.375\ell\chi_e\mathcal{R}(\chi_e)}{1+0.574\chi_e^{2/3}}. \tag{14}$$

Considering that the prefactor $\alpha a_0 n_{\mathrm{eff}} \sim O(1)$ for near-term experimental parameters, this may be used for an order-of-magnitude estimate for the number of positrons per electron. For $\ell \sim 0.1$ and $\chi_e \sim 1$, $\mathcal{B} \sim 10^{-3}$. Thus if the bremsstrahlung photons from a few picocoulombs of accelerated electrons reach the laser focal spot, we can expect thousands of Breit–Wheeler positrons to be produced.

To verify this, we use GEANT4 to simulate the interaction of an electron beam with a solid target, then take the resultant photon spectrum as input to CIRCE [20, 36], a single-particle Monte Carlo code that simulates strong-field QED cascades in intense laser pulses. It does this by factorizing the cascade into a product of first-order processes (nonlinear Compton scattering and Breit–Wheeler pair creation), which occur along the particle trajectory at locations pseudorandomly determined according to the appropriate LCFA probability rate. (See [45, 46] for detailed discussion of this 'QED-PIC' concept.)

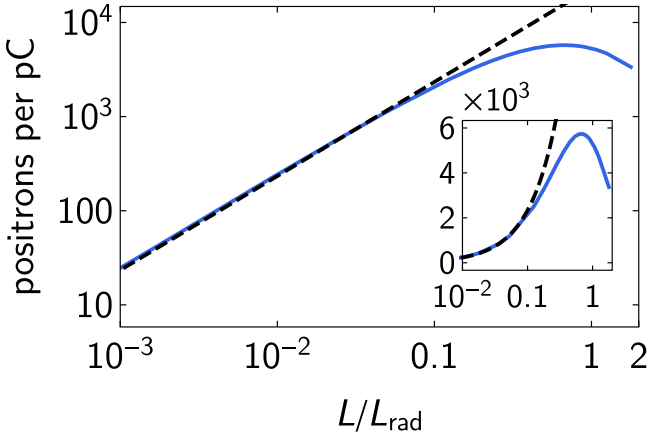

Figure 5. The number of positrons per pC of charge in the electron beam, when the bremsstrahlung photons it produces in a lead target with thickness L collide with a laser pulse that has $a_0 = 30$ and $n_{\mathrm{eff}} = 15$: (blue, solid) from simulations, (black, dashed) as predicted by (14).

We compare the positron yield predicted by (12) and (14) and by simulations in figure 5. The electron beam energy is 2 GeV, and all the bremsstrahlung photons it produces in a lead target collide head-on with a laser pulse that has $a_0 = 30$, duration $\tau = 40$ fs and wavelength 0.8 μm, i.e. $n_{\mathrm{eff}} = 15$. We see that for $\ell < 0.1$, the positron yield increases linearly with target thickness, in good agreement with (14). As ℓ continues to increase, the yield reaches a maximum of 5×10^3 at $\ell = 0.7$ and then begins to decrease. This is

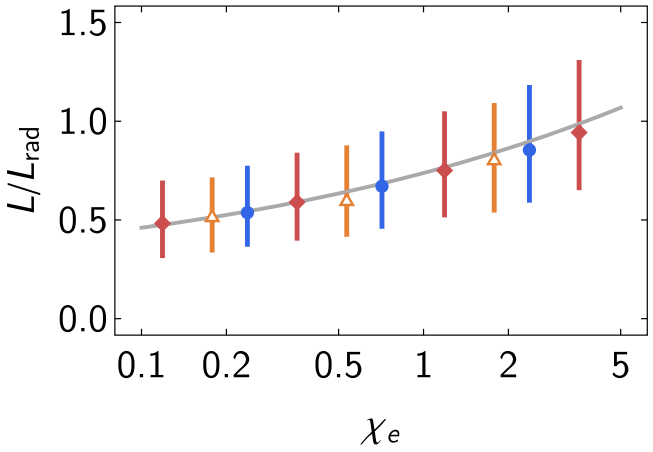

Figure 6. The target thickness L per unit radiation length $L_{\rm rad}$ which maximizes Breit–Wheeler pair creation when the bremsstrahlung photons collide with an intense laser pulse: (grey) as predicted by (15) and (points) from simulations in which (blue) 2 GeV electrons hit a lead target, (orange) 1.5 GeV electrons hit copper and (red) 1 GeV electrons hit tantalum. Vertical bars indicate the range of $L/L_{\rm rad}$ over which the Breit–Wheeler positron yield is at least 95% of maximum.

readily explained as the effect of pair creation within the solid target, which causes attenuation of the high-energy part of the photon spectrum. As it is these photons that are most likely to pair create, increasing ℓ eventually causes the Breit–Wheeler positron yield to decrease.

If we use (9) rather than (8) to model the photon spectrum, then we may predict the ℓ which maximizes the yield of Breit–Wheeler positrons. This is given by the root of the following integral equation:

$$\int_0^1 \mathcal{R}(f\chi_e)\frac{\partial^2 N_\gamma}{\partial \ell \partial f}\,\mathrm{d}f = 0, \tag{15}$$

where the double differential photon spectrum is obtained from (9). For convenience we solve this numerically for a range of χ_e and fit a two-component power law to the results. We find that the optimal thickness $\ell_{\rm opt} \simeq 0.693\chi_e^{1/4} + 0.0447\chi_e^{-1/5}$ for $0.01 < \chi_e < 10$, over which range the fit is accurate to 0.5%. As an example, if $\chi_e = 0.71$ as in figure 5, (15) predicts that the positron yield is maximized at $\ell = 0.68$. This is in good agreement with the simulation results, where we find $\ell_{\rm opt} = 0.67$.

Further verification of (15) is shown in figure 6. Each point represents the optimal ℓ found from a set of simulations in which the target thickness is varied, while the electron beam energy E_0, target material, and laser amplitude a_0 remain fixed. The materials under consideration are lead, copper and tantalum, which have radiation lengths of 5.61 mm, 14.4 mm and 4.09 mm respectively. The laser a_0 is one of 10, 30 and 100 and $n_{\rm eff} = 15$ for all scans. Our analytical prediction agrees well with the simulation results across a broad range of electron beam and target parameters.

We find that the optimal target thickness increases only slowly with increasing χ_e. Furthermore, the width of this maximum, indicated by vertical lines in figure 6, is large. Therefore across the whole range $0.1 < \chi_e < 10$, a positron yield close to maximum can be obtained simply by setting $\ell \simeq 0.7$. This is well within expectations, as the radiation length is approximately the distance over which one photon or electron–positron pair is added to the QED cascade in the material. Keeping $\ell \lesssim 1$ ensures that there are sufficient high-energy photons emitted while minimizing Bethe–Heitler pair creation.

This result further indicates that no special treatment is required for electron beams with broad energy spectra, i.e. a large spread in χ_e. If $\ell \simeq 0.7$, the target thickness is close to optimized for all components of the beam but the low-energy tail, which contributes negligibly to pair creation. Provided that there are picocoulombs of electrons with $E_0 > 2$ GeV, then as shown in figure 5, we expect thousands of positrons to be produced in a laser pulse with $a_0 = 30$, i.e. a peak intensity of 2×10^{21} W cm^{-2}.

5. Summary

In this paper we have discussed the prospects for experimental observation of nonlinear Breit–Wheeler pair creation, using the collision between an intense laser pulse and the γ rays produced by bremsstrahlung of a LWFA electron beam in a high-Z target. We have shown that the thickness of the high-Z target L may be optimized to maximize the number of Breit–Wheeler positrons: across a broad range of experimentally accessible parameters, this is $L/L_{\rm rad} = 0.7$, where $L_{\rm rad}$ is the radiation length.

However, we found that even though the divergence of the γ ray beam is small, it is sufficient to cause most of the photons to miss the laser focal spot. This due to transverse broadening of the γ ray beam as it traverses the spatial separation between the solid target and the focal plane of the laser pulse. (This separation is required for magnetic deflection of the source electrons and background electron–positron pairs.) As suggested in [16], this makes it necessary to focus the electron beam before it hits the high-Z target. Provided that this is done, the bremsstrahlung spectrum of a multi-GeV electron beam with picocoulombs of charge is sufficiently hard for thousands of positrons to be produced in the intense laser pulse.

Acknowledgments

The authors thank S Yoffe and A Noble for useful discussions and acknowledge support from the Knut and Alice Wallenberg Foundation and the Swedish Research Council (grants 2013-4248 and 2016-03329). Simulations were performed on resources provided by the Swedish National Infrastructure for Computing (SNIC) at the High Performance Computing Centre North (HPC2N).

ORCID iDs

T G Blackburn https://orcid.org/0000-0002-3681-356X

M Marklund https://orcid.org/0000-0001-9051-6243

References

[1] Breit G and Wheeler J A 1934 *Phys. Rev.* **46** 1087–91
[2] Burke D L *et al* 1997 *Phys. Rev. Lett.* **79** 1626–9
[3] Bula C *et al* 1996 *Phys. Rev. Lett.* **76** 3116–9
[4] Heinzl T and Ilderton A 2009 *Opt. Commun.* **282** 1879–83
[5] Timokhin A N 2010 *Mon. Not. R. Astron. Soc.* **408** 2092–114
[6] Bell A R and Kirk J G 2008 *Phys. Rev. Lett.* **101** 200403
[7] Esarey E, Schroeder C B and Leemans W P 2009 *Rev. Mod. Phys.* **81** 1229–85
[8] Kim H T, Pae K H, Cha H J, Kim I J, Yu T J, Sung J H, Lee S K, Jeong T M and Lee J 2013 *Phys. Rev. Lett.* **111** 165002
[9] Wang X *et al* 2013 *Nat. Commun.* **4** 1988
[10] Leemans W P *et al* 2014 *Phys. Rev. Lett.* **113** 245002
[11] Bahk S W, Rousseau P, Planchon T A, Chvykov V, Kalintchenko G, Maksimchuk A, Mourou G A and Yanovsky V 2004 *Opt. Lett.* **29** 2837–9
[12] Kiriyama H *et al* 2017 10^{22} W cm^{-2}, 0.1 Hz J-KAREN-P laser facility at qst *Conf. on Lasers and Electro-Optics* (Optical Society of America) p SF1K.2 (http://osapublishing.org/abstract.cfm?URI=CLEO_SI-2017-SF1K.2)
[13] Bulanov S V *et al* 2011 *Nucl. Instrum. Methods Phys. Res.* A **660** 31–42
[14] Cole J M *et al* 2018 *Phys. Rev.* X **8** 011020
[15] Poder K *et al* 2017 arXiv:1709.01861
[16] Turcu I *et al* 2016 *Rom. Rep. Phys.* **68** S145–231
[17] Ledingham K W D and Galster W 2010 *New J. Phys.* **12** 045005
[18] Albert F and Thomas A G R 2016 *Plasma Phys. Control. Fusion* **58** 103001
[19] Ritus V I 1985 *J. Sov. Laser Res.* **6** 497–617
[20] Blackburn T G, Ilderton A, Murphy C D and Marklund M 2017 *Phys. Rev.* A **96** 022128
[21] Tsai Y S 1974 *Rev. Mod. Phys.* **46** 815–51
[22] Pike O J, Mackenroth F, Hill E G and Rose S J 2014 *Nat. Photon.* **8** 434–6
[23] Ribeyre X, d'Humières E, Jansen O, Jequier S, Tikhonchuk V T and Lobet M 2016 *Phys. Rev.* E **93** 013201
[24] Tang S, Bake M A, Wang H Y and Xie B S 2014 *Phys. Rev.* A **89** 022105
[25] Erber T 1966 *Rev. Mod. Phys.* **38** 626–59
[26] Baier V N, Katkov V M and Strakhovenko V M 1998 *Electromagnetic Processes at High Energies in Oriented Single Crystals* (Singapore: World Scientific)
[27] Dinu V, Harvey C, Ilderton A, Marklund M and Torgrimsson G 2016 *Phys. Rev. Lett.* **116** 044801
[28] Krajewska K and Kamiński J Z 2012 *Phys. Rev.* A **86** 052104
[29] Nousch T, Seipt D, Kämpfer B and Titov A I 2012 *Phys. Lett.* B **715** 246–50
[30] Titov A I, Kämpfer B, Takabe H and Hosaka A 2013 *Phys. Rev.* A **87** 042106
[31] Meuren S, Hatsagortsyan K Z, Keitel C H and Di Piazza A 2015 *Phys. Rev.* D **91** 013009
[32] Di Piazza A 2016 *Phys. Rev. Lett.* **117** 213201
[33] Jirka M, Klimo O, Vranic M, Weber S and Korn G 2017 *Sci. Rep.* **7** 15302
[34] Salamin Y I 2007 *Appl. Phys.* B **86** 319–26
[35] Samarin G M, Zepf M and Sarri G 2017 *J. Mod. Opt.* **64** 2281–8
[36] Blackburn T G 2015 *Plasma Phys. Control. Fusion* **57** 075012
[37] Sarri G *et al* 2013 *Plasma Phys. Control. Fusion* **55** 124017
[38] Compant La F A, Courtois C and Lefebvre E 2012 *Phys. Plasmas* **19** 023104
[39] Avetissian H K, Matevosyan H H, Mkrtchian G F and Sedrakian K V 2015 *Phys. Rev. Spec. Top. Accel. Beams* **18** 121301
[40] Avetissian H K 2016 *Relativistic Nonlinear Electrodynamics* 2nd edn (New York: Springer)
[41] Bethe H and Heitler W 1934 *Proc. R. Soc.* A **146** 83–112
[42] Agostinelli S *et al* 2003 *Nucl. Instrum. Methods Phys. Res.* A **506** 250–303
[43] Allison J *et al* 2006 *IEEE Trans. Nucl. Sci.* **53** 270–8
[44] Allison J *et al* 2016 *Nucl. Instrum. Methods Phys. Res.* A **835** 186–225
[45] Ridgers C P, Kirk J G, Duclous R, Blackburn T G, Brady C S, Bennett K, Arber T D and Bell A R 2014 *J. Comput. Phys.* **260** 273–85
[46] Gonoskov A, Bastrakov S, Efimenko E, Ilderton A, Marklund M, Meyerov I, Muraviev A, Sergeev A, Surmin I and Wallin E 2015 *Phys. Rev.* E **92** 023305